

Supporting Information

Reversible maleimide-thiol adducts yield glutathione-sensitive poly(ethylene glycol)-heparin hydrogels

Aaron D. Baldwin¹, Kristi L. Kiick^{1,2}

¹Department of Materials Science and Engineering, 201 DuPont Hall, University of Delaware, Newark, DE 19716, USA

²Delaware Biotechnology Institute, 15 Innovation Way, Newark, DE 19716, USA

Table of Contents

¹ H-NMR Spectra of synthesized compounds	3
Figure S1. ¹ H-NMR spectrum for four arm thiolated PEG esterified with 3-mercaptopropionic acid (PEG-MP).....	3
Figure S2. ¹ H-NMR spectrum for four arm thiolated PEG esterified with 4-mercaptophenylpropionic acid (PEG-MPP).....	4
Figure S3. ¹ H-NMR spectrum for four arm thiolated PEG esterified with 3-mercaptopropionic acid (PEG-MIB).....	5
Figure S4. ¹ H-NMR spectrum for four arm thiolated PEG esterified with 2,2-dimethyl-3-(4-mercaptophenyl)propionic acid (PEG-DMMPP).....	6
Figure S5. ¹ H-NMR spectrum for compound maleimide functionalized LMWH (Mal-LMWH) $f \approx 2.6$	7
Hydrogel Degradation monitored by Oscillatory Rheology	7
Figure S6. Representation of the rheometer setup enabling measurement of hydrogel moduli over extended periods of time without buffer evaporation.	7
Oscillatory Rheology	8
Figure S7. Time-sweep and frequency-sweep plots for PEG-LMWH hydrogels for all PEG-thiol functionalities.....	8
Hydrogel Elasticity Compared With Rubber Elasticity Theory	9
¹ H-NMR Monitoring of Hydrogel Formation.....	9
Figure S8. ¹ H-NMR analysis of the formation of (a) PEG-MP and (b) PEG-MPP containing PEG-LMWH hydrogels.....	10
PEG-Thiol Auto-oxidation.....	10
Figure S9. Free thiol content comparison for PEG-MPP (▲) and PEG-MP (●) as determined by Ellman's assay.....	11
Hydrogel Degradation Kinetics	11
Figure S10. The number of effective crosslinking strands depends heavily on the functionality (f) of the LMWH. A $f=2$ produces one effective strand between the PEG crosslink with two GSH-sensitive linkages between centers, while a $f=3$ produces three effective strands between the PEG crosslink with one GSH-sensitive linkage between each center.....	12
Figure S11. Comparison of the degrading storage moduli for hydrogels most sensitive to reducing conditions	13
References.....	Error! Bookmark not defined.

¹H-NMR Spectra of synthesized compounds

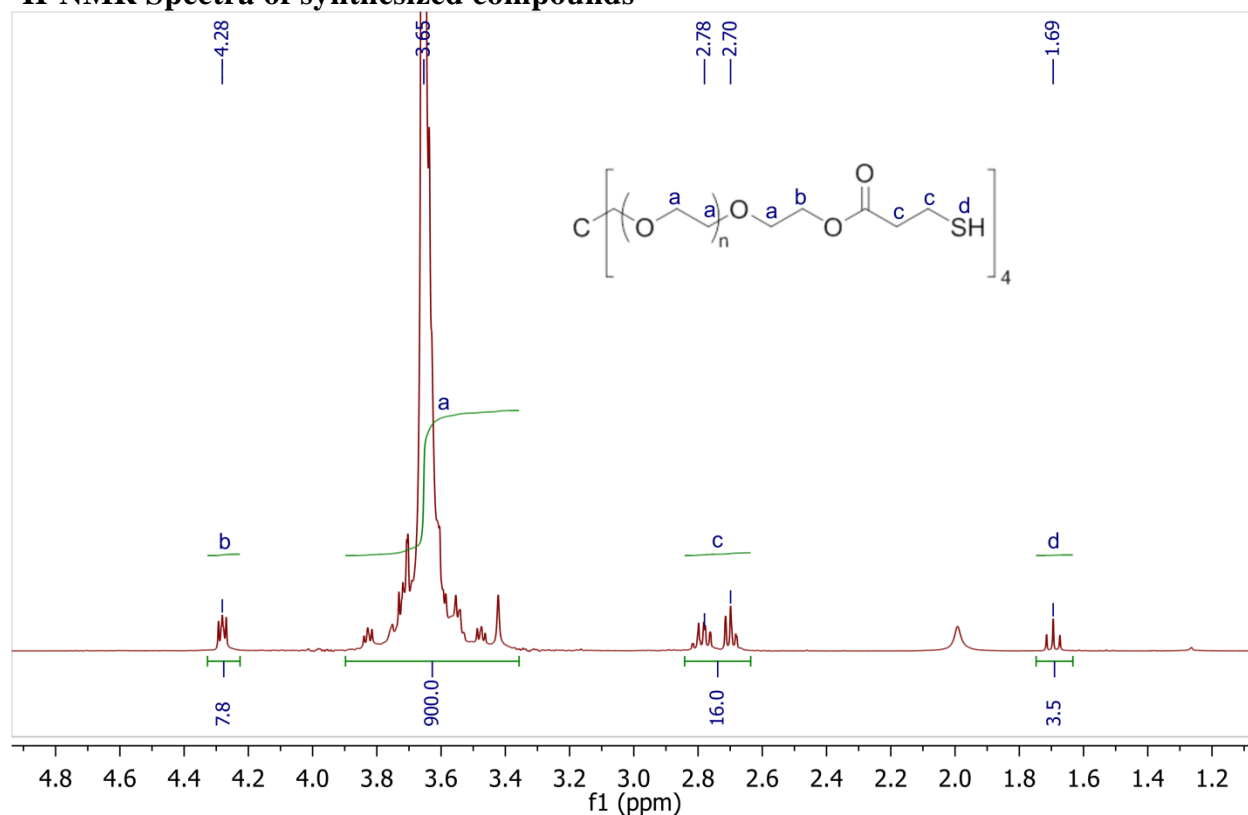


Figure S1. ¹H-NMR spectrum for four arm thiolated PEG esterified with 3-mercaptopropionic acid (PEG-MP). Functionality calculated based on the integration of the proton neighboring the ester (b), in this case 98% functional.

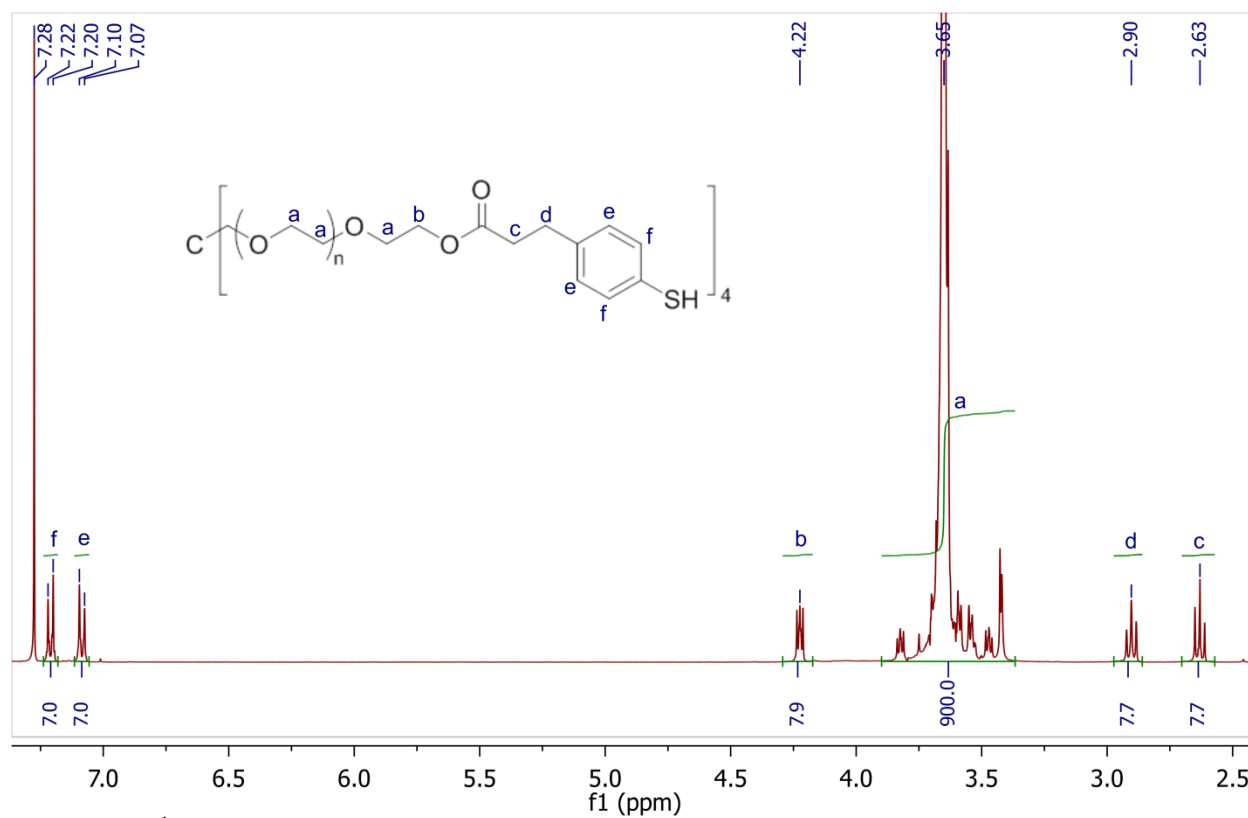


Figure S2. ¹H-NMR spectrum for four arm thiolated PEG esterified with 4-mercaptophenylpropionic acid (PEG-MPP).

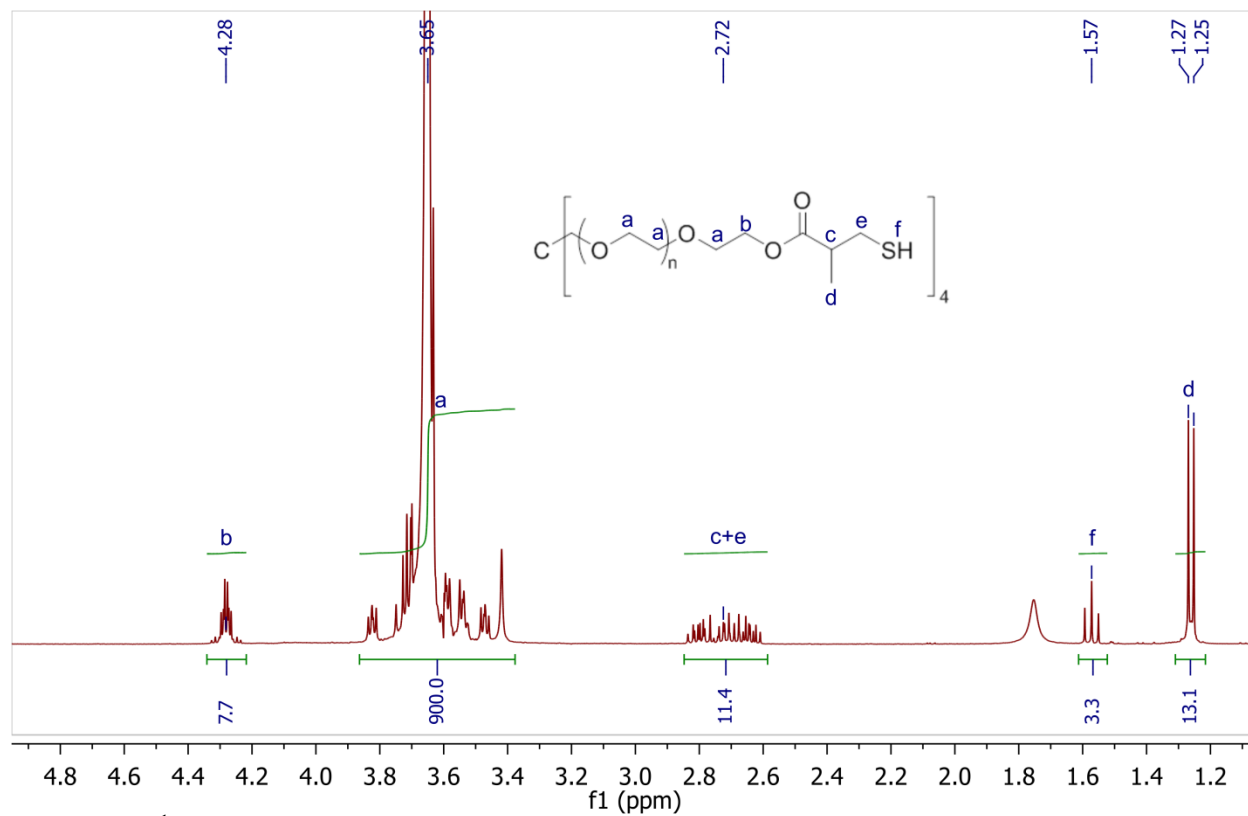


Figure S3. $^1\text{H-NMR}$ spectrum for four arm thiolated PEG esterified with 3-mercaptopisobutyric acid (PEG-MIB).

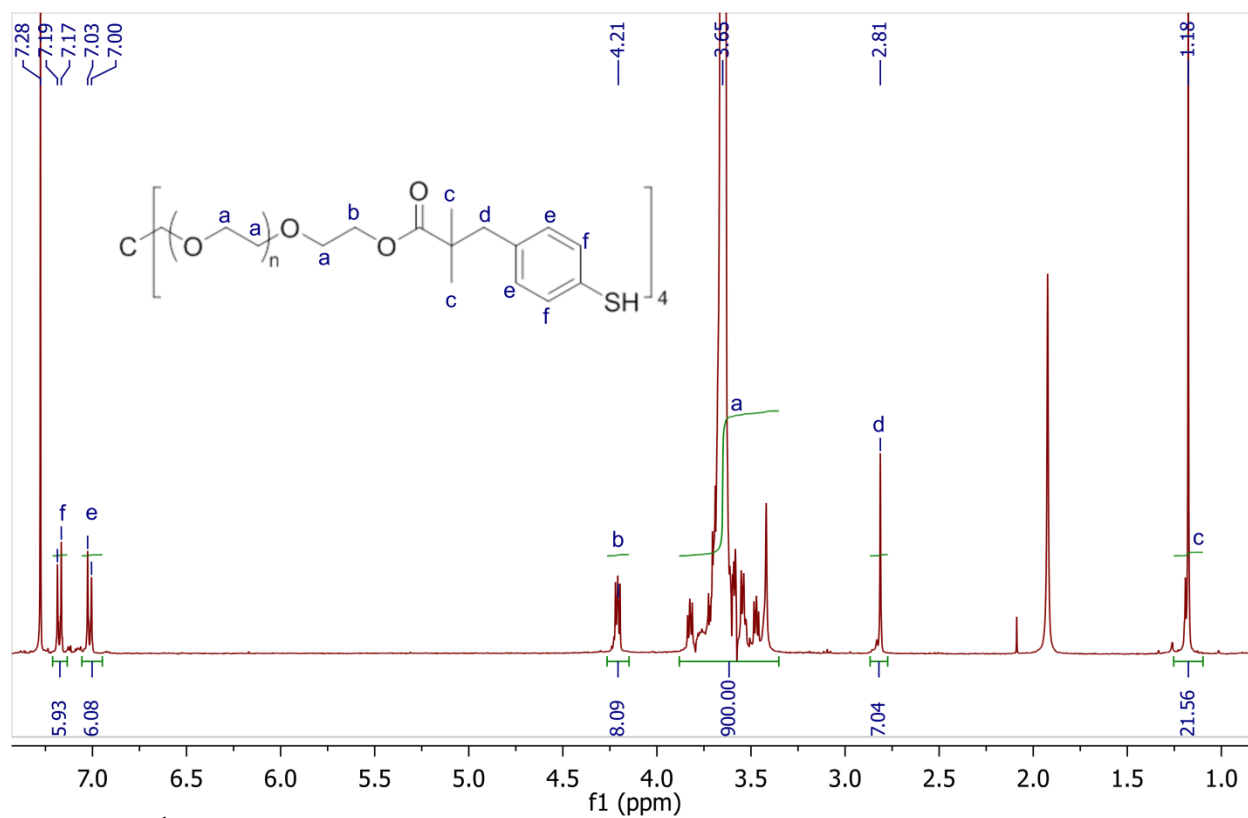


Figure S4. ¹H-NMR spectrum for four arm thiolated PEG esterified with 2,2-dimethyl-3-(4-mercaptophenyl)propionic acid (PEG-DMMPP).

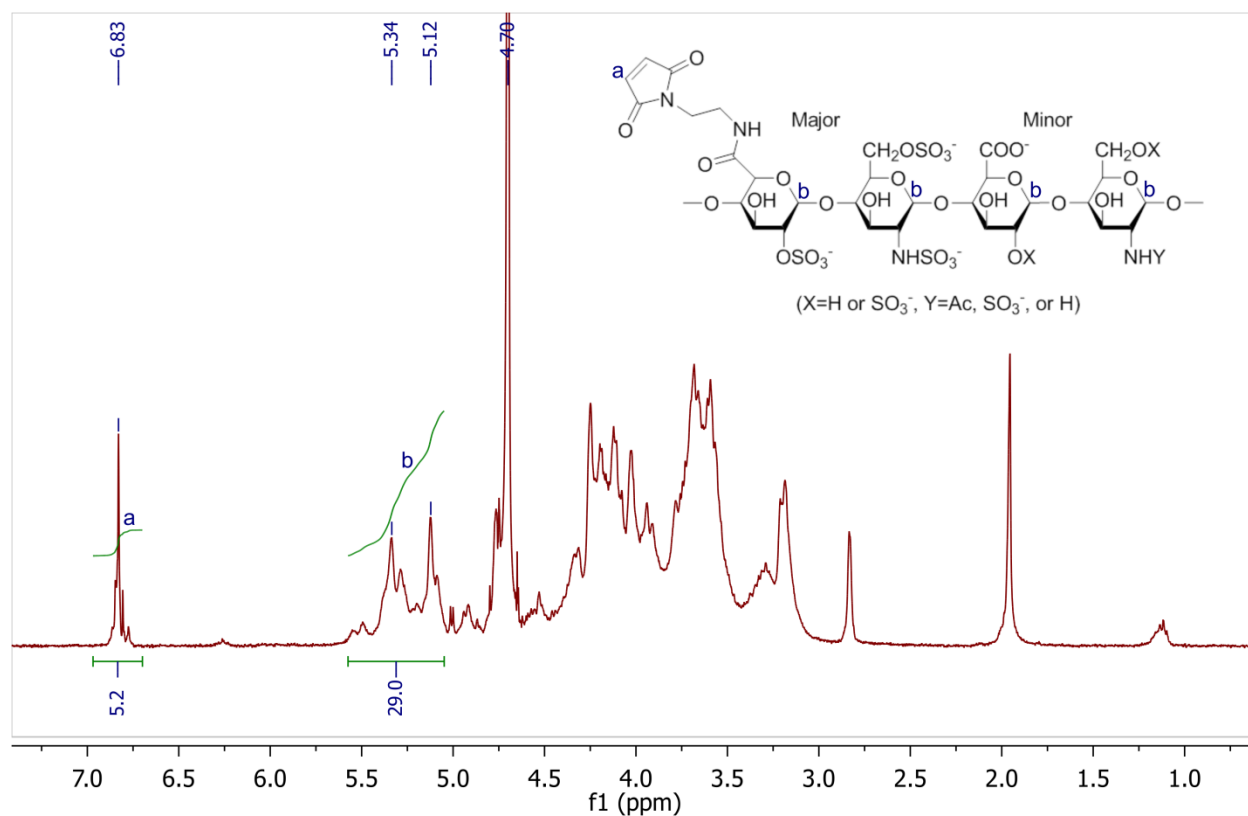


Figure S5. ¹H-NMR spectrum for compound maleimide functionalized LMWH (Mal-LMWH) $f \approx 2.6$. Maleimide peaks (a) appear at 6.83ppm. Anomeric protons of LMWH (b) were assumed to appear at chemical shift values between 5.60-5.05ppm (29H).

Hydrogel Degradation monitored by Oscillatory Rheology

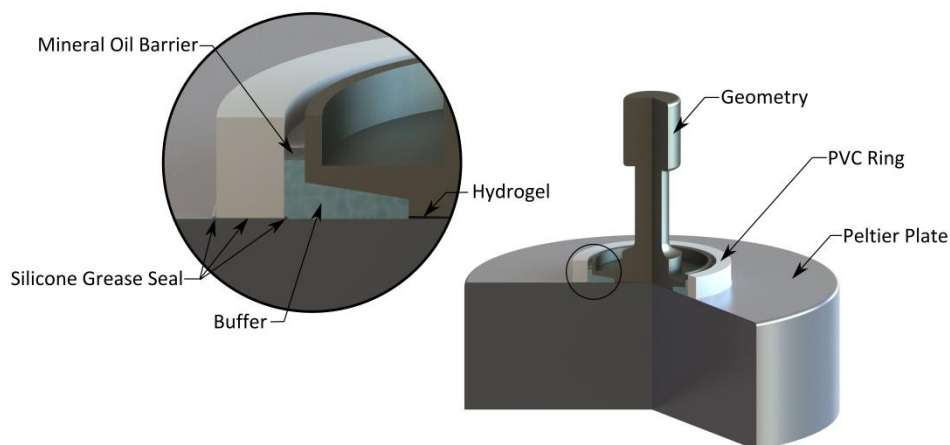


Figure S6. Representation of the rheometer setup enabling measurement of hydrogel moduli over extended periods of time without buffer evaporation.

Oscillatory Rheology

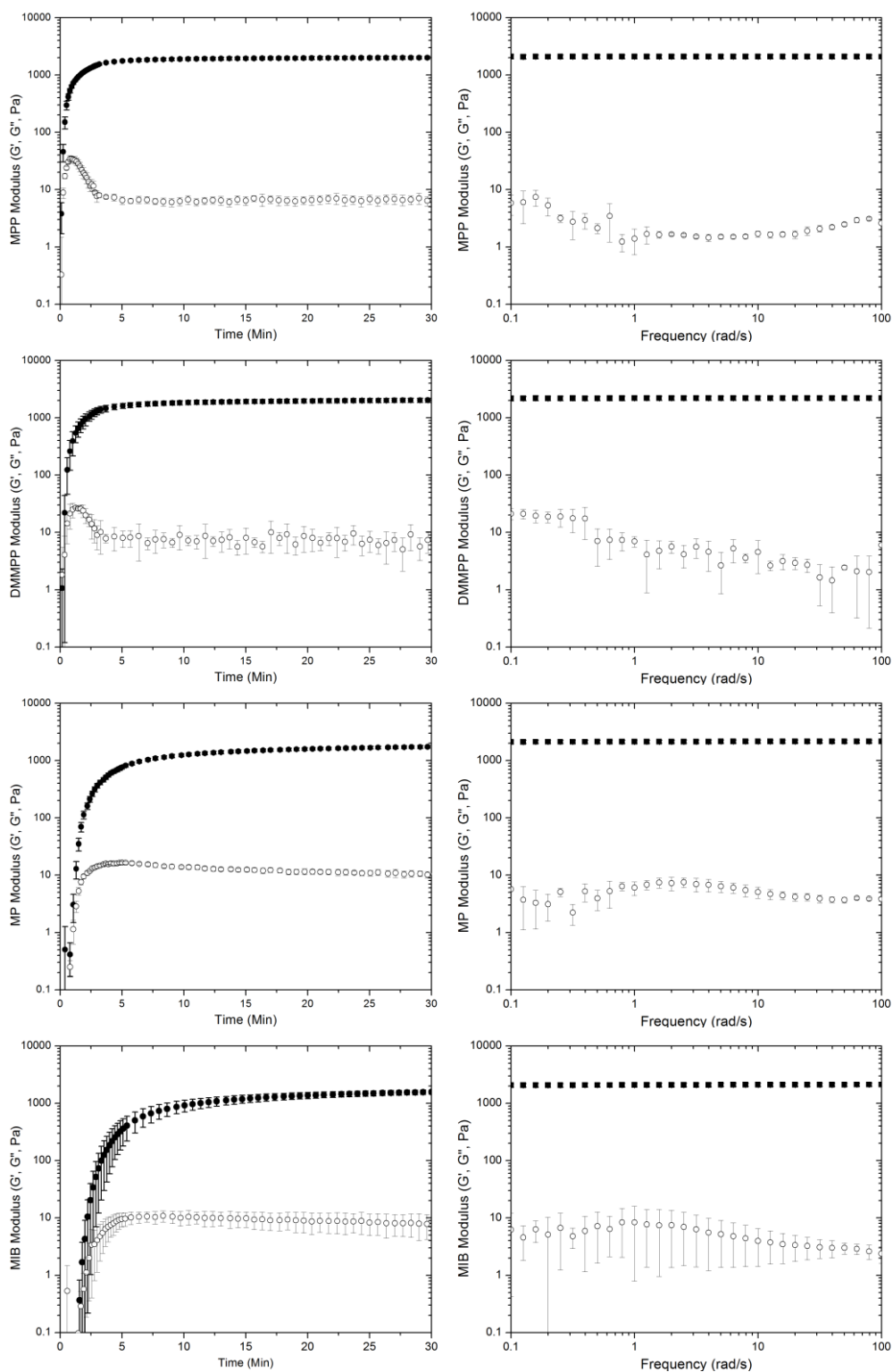


Figure S7. Time-sweep and frequency-sweep plots for PEG-LMWH hydrogels for all PEG-thiol functionalities. Row: 1) PEG-MPP; 2) PEG-DMMPP; 3) PEG-MP; 4) PEG-MIB. Closed symbols indicate G' while open symbols indicate G'' . Error bars represent the standard deviation of the results of three separate runs. All hydrogels are highly elastic with $G' \gg G''$.

Hydrogel Elasticity Compared With Rubber Elasticity Theory

The theoretically predicted maximum storage modulus for these hydrogels can be calculated using classical rubber elasticity theory as shown in equation S1.¹

$$G = RT \frac{\nu_e}{V} \quad (\text{S1})$$

Here, R is the gas constant, T is absolute temperature, and ν_e/V represents the total moles of elastically effective strands per volume. In the hydrogel system described here, an ideal scenario would produce an average of 7.4 moles of active strands per cubic meter, equating to a theoretically predicted maximum storage modulus of 19.1 kPa at 37°C. This simplistic equation neglects for the hydration of the network and for network features such as loops, chain entanglements, and chain ends, however, the average modulus of all hydrogels (ca. 2.1kPa) is only ~11% of the theoretical maximum, indicating that these gels formed in dilute concentrations (5wt%) facilitates an inefficient network formation.

¹H-NMR Monitoring of Hydrogel Formation

PEG-thiols and Mal-LMWH were dissolved separately in deuterated PBS, mixed and loaded into a small capillary tube before the onset of gelation. The capillary tubes were then submerged in NMR tubes containing deuterated PBS and monitored via NMR at room temperature. Data for two representative thiol-functionalized PEGs, PEG-MP and PEG-MPP, are shown for these experiments in Figure S8, with resulting spectra for each hydrogel given over time. The presence of both the PEG and LMWH complicated some spectral assignments, especially in overlapping regions of the PEG and LMWH from 2.7 to 5.6ppm; however, a few key spectral changes could be assigned for each hydrogel type. The crosslinking of the PEG-MP containing hydrogel (Figure S8a) proceeded at rates slow enough that the disappearance of the maleimide protons (6.82ppm) and methylene protons neighboring the thiol substituent (centered at 2.7ppm) could be monitored with time. The peaks from the maleimide protons fully disappeared, along with the neighboring thiol methylene protons, within 1h, indicating that the Michael-type addition between the thiol moieties and maleimide was complete. The apparent absence of the resonances from the succinimide thioether protons is likely a result of their coincidence with other LMWH peaks. The spectra remained unchanged from 1 hour to 5 days (data not shown).

The gelation of the PEG-MPP with Mal-LMWH proceeded at accelerated rates compared with those of the PEG-MP-containing hydrogels, attributed to the lower pKa of the aromatic thiol versus an alkyl thiol. The rapid reaction kinetics prevented capture of the reduction of the maleimide proton intensity in these NMR experiments (spectral changes were complete in 10 minutes). However, the spectral differences between starting materials and resulting hydrogels are shown for comparison in Figure S8b. Here, the individual sharp peaks of the phenylthiol ring (centered at 7.0 and 7.2ppm, trace 1) and methylene protons of MPP (centered at 2.6ppm and 2.8ppm, trace 2) are broadened and shift downfield upon crosslinking (to 7.2 and 7.4ppm and to 2.7 and 2.9ppm, trace 3), with no peaks from residual unreacted materials. As in the PEG-MP-containing gels, the peak from the maleimide protons (6.8ppm, trace 2) disappears completely after mixing (trace 3). Although solid state or magic angle spinning NMR techniques are normally used to obtain quantifiable spectra from hydrogels,²⁻⁵ here we show a reduction in peak intensity (by line broadening) over the course of the experiment, while the integration of the LMWH peaks maintain near unity, thus both the soluble and gel fraction are measured in the experiment. This ability to monitor the crosslinking reaction with standard solution phase NMR techniques may be attributable to the highly

anionic nature of heparin, which would serve to increase the solubility and molecular motion of the polymer chains in these hydrogels.

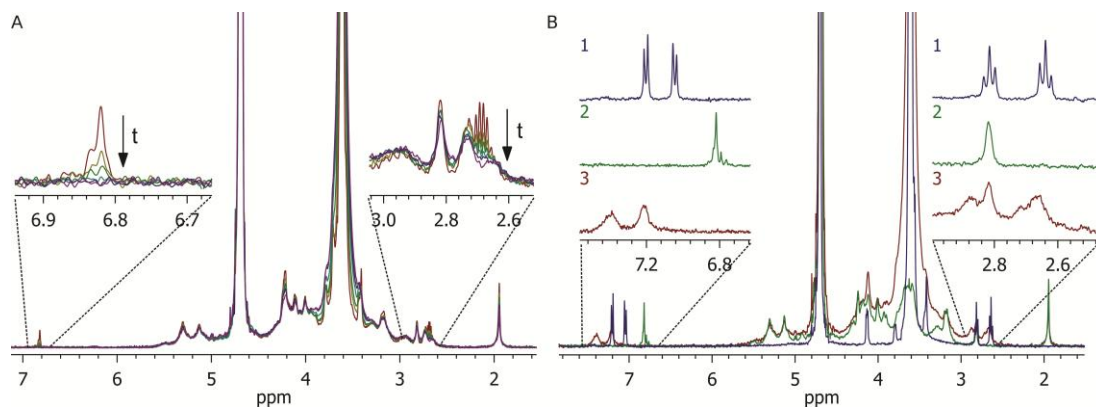


Figure S8. $^1\text{H-NMR}$ analysis of the formation of (a) PEG-MP and (b) PEG-MPP containing PEG-LMWH hydrogels. The maleimide peak (6.82ppm) disappeared within 1 hour for PEG-MP (arrow indicates increasing time) and in less than 10 minutes for PEG-MPP containing hydrogels. The fast gelation kinetics of PEG-MPP prevented the analysis of the disappearance of the maleimide peak, for reference trace 1= PEG-MPP starting material, 2= Mal-LMWH starting material, 3= final hydrogel showing no resonances from the maleimide protons and broad resonances from the phenylthiol and methylene protons.

PEG-Thiol Auto-oxidation

Standard Ellman's assay protocols were used. Briefly, standard solutions were made of thiol-functionalized PEG were dissolved in PBS pH 7.4 at concentrations that would be used in hydrogel precursor solutions (ie 2.0mg/100 μL for 5wt% hydrogels). Solutions were stored at room temperature, without agitation, and free to the atmosphere. 10 μL samples were collected at 2, 6, 24, 48 hours and 5 days. Each sample was immediately diluted with 50 μL of 2mM 5,5'-dithiobis(2-nitrobenzoic acid) (DTNB, Sigma-Aldrich, St. Louis, MO, USA) pre-dissolved in 50mM sodium acetate (Fisher Scientific, Pittsburgh, PA, USA) and 940 μL of 0.1M pH 8.0 tris(hydroxymethyl)aminomethane (TRIS, Fisher Scientific). Solutions were mixed and incubated for 5 minutes before measuring the absorbance using an Agilent 8453 spectrophotometer (Santa Clara, CA, USA) in a Hellma 3mm quartz cuvette (Plainview, NY, USA). The spectrophotometer was blanked with solution composed of the 50 μL DTNB solution diluted with 950 μL TRIS buffer.

The free thiol content for the measured samples is shown in Figure S10. The oxidation of thiols is a complex reaction with catalysis occurring from trace metals contained in solution, though the oxidation can be approximated to be zero order.⁶ In this case the half-lives are 13.5 hours and 4.7days for PEG-MPP and PEG-MP. PEG-MIB and PEG-DMMPP were assumed to have similar kinetics as PEG-MPP and were not studied here.

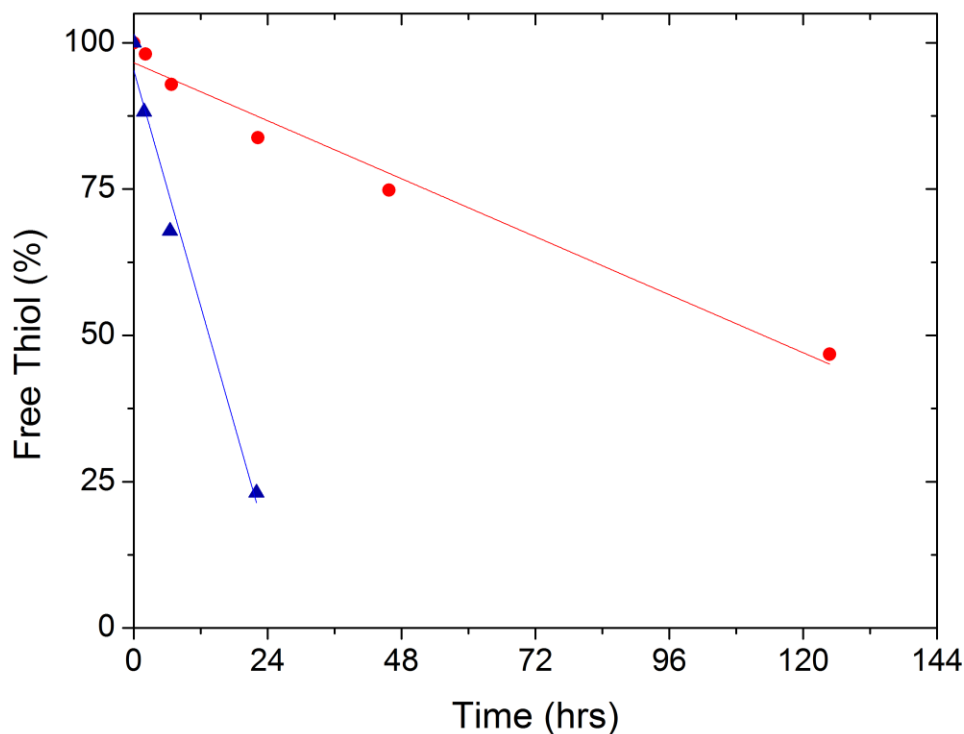


Figure S9. Free thiol content comparison for PEG-MPP (▲) and PEG-MP (●) as determined by Ellman's assay.

Hydrogel Degradation Kinetics

The degradation profiles can be evaluated via standard rubber elasticity theory in conjunction with the rate of scission of any network active chain. In the case of the disulfide gel, we assume that the cleavage of the disulfide is based on pseudo-first order kinetics (equation S2):

$$\frac{d[SS]}{dt} = -k'[SS] \quad (S2)$$

Where the [SS] is the concentration of disulfides, and k' is the pseudo first-order reaction rate constant. Integration of equation S2 gives us the concentration of disulfides within the gel as a function of time:

$$[SS] = [SS]_0 e^{-k't} \quad (S3)$$

The structure of the crosslinked disulfide network has one disulfide between each junction point; therefore, the crosslinking density or (ρ_c) is directly proportional the amount of remaining disulfides or $[SS]/[SS]_0$ and we arrive at equation S4.

$$\rho_c \propto e^{-k't} \quad (S4)$$

With the knowledge of classical rubber elasticity theory (equation S1), where the storage modulus (G) is proportional to the total moles of elastically effective strands per volume (ν_e/V) or ρ_c we can further generalize equation S5 where the storage modulus is proportional to the exponential of pseudo first-order cleavage reaction.¹

$$G \propto \rho_c \propto e^{-k't} \quad (\text{S5})$$

Following suit, a similar generalization can be made for the retro-Michael addition hydrogels, however, each multifunctional crosslink is not as well defined as in the above four-arm star disulfide polymer, with the average functionality of the LMWH equating 2.6. Thus, each crosslink may contain a single glutathione-sensitive linkage between a polymer junction point or two depending on the functionality of the LMWH reacted with the PEG (Scheme S1). Consequently, the number of GSH-sensitive linkages does not directly equate to the number of ν_e . To correct for this fact in calculations of the average functionality, we must correct for the linkages with functionality less than three (equation S6).

$$F_{cp} = \frac{n \cdot f - n \cdot (3-f)}{n \cdot f} \quad (\text{S6})$$

Where the fraction of crosslinking points (F_{cp}) (of the total number of GSH-sensitive linkages) is equal to the number of moles LMWH (n) · functionality (f) minus the number of GSH-sensitive linkages that have a functionality of less than three ($n \cdot (3-f)$), over the total number GSH-sensitive linkages.



Figure S10. The number of effective crosslinking strands depends heavily on the functionality (f) of the LMWH. A $f=2$ produces one effective strand between the PEG crosslink with two GSH-sensitive linkages between centers, while a $f=3$ produces three effective strands between the PEG crosslink with one GSH-sensitive linkage between each center.

At a LMWH functionality of 2.6, F_{cp} is 0.85, therefore the pseudo-first order kinetic parameter derived from the first order fit from the modulus (k'_{mod}) would overestimate the actual pseudo-first order kinetic parameter for GSH-sensitive linkages (k') by the factor of F_{cp} , or more simply:

$$k' = 0.85k'_{mod} \quad (\text{S7})$$

Fitting the entire curve of the disulfide sensitive hydrogel and the first 15 hours of the retro-Michael addition hydrogels (thus neglecting ring opening of the succinimide thioether) to an exponential decay yielded high coefficients of determination (>0.99) (Figure S9). Fitting the entire curve of the disulfide sensitive hydrogels yielded pseudo-first order constants of $0.81 \pm 0.1 \text{ h}^{-1}$. To obtain degradation constants for the retro-Michael addition further manipulation was necessary to neglect for hydrolysis of the ester. Hydrolysis constants were determined by oscillatory rheology by swelling the PEG-LMWH hydrogels under standard reducing conditions. Approximate pseudo-first order hydrolysis constants were 0.014 h^{-1} for PEG-MPP and 0.010 h^{-1} for PEG-DMMPP containing PEG-LMWH hydrogels. Negating for hydrolysis and correcting for the functionality of LMWH as discussed above, the pseudo-first order are calculated to be $0.039 \pm 0.006 \text{ h}^{-1}$ for PEG-MPP and $0.031 \pm 0.003 \text{ h}^{-1}$ for PEG-DMMPP containing PEG-LMWH hydrogels.

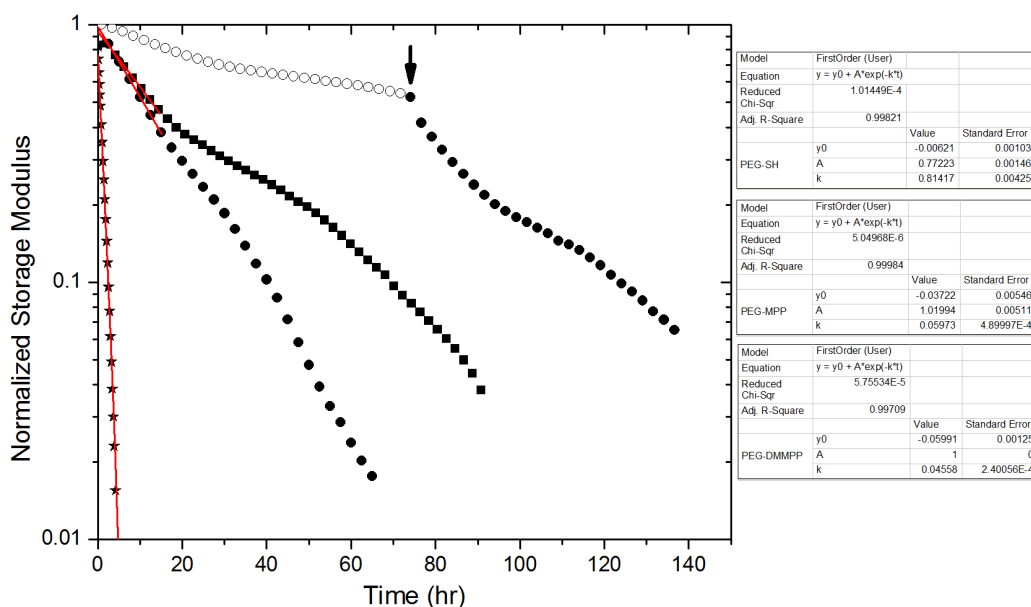


Figure S11. Comparison of the degrading storage moduli for hydrogels most sensitive to reducing conditions: PEG-SH hydrogel (★) LMWH-PEG-MPP (●) and -DMMPP (■) under high reducing conditions (10mM GSH) and LMWH-PEG-MPP (□) under standard reducing conditions (10 μ M GSH). At 72 h (arrow) the buffer of the standard reducing condition hydrogel was exchanged for high reducing buffer, showing an increase in rate of degradation. Free thiol content comparison for PEG-MPP (▲) and PEG-MP (●) as determined by Ellman's assay. Derived fits to a first order exponential shown to the right.

References

1. P. C. Hiemenz and T. Lodge, *Polymer chemistry*, CRC Press, Boca Raton, Fla., 2007.
2. T. Pouyani, G. S. Harbison and G. D. Prestwich, *Journal of the American Chemical Society*, 1994, **116**, 7515-7522.
3. S. J. Bryant, K. A. Davis-Arehart, N. Luo, R. K. Shoemaker, J. A. Arthur and K. S. Anseth, *Macromolecules*, 2004, **37**, 6726-6733.

4. D. Capitani, A. A. De Angelis, V. Crescenzi, G. Masci and A. L. Segre, *Carbohydrate Polymers*, 2001, **45**, 245-252.
5. E. Díez-Peña, I. Quijada-Garrido, J. M. Barrales-Rienda, I. Schnell and H. W. Spiess, *Macromolecular Chemistry and Physics*, 2004, **205**, 430-437.
6. G. A. Bagiyan, I. K. Koroleva, N. V. Soroka and A. V. Ufimtsev, *Russian Chemical Bulletin*, 2003, **52**, 1135-1141.